Dynamic crossovers and activated regimes in a narrow distribution poly(n-butyl acrylate): an ESR study

2006 J. Phys.: Condens. Matter 18 6481

(http://iopscience.iop.org/0953-8984/18/28/004)

INSTITUTE OF PHYSICS PUBLISHING JOURNAL OF PHYSICS: CONDENSED MATTER

J. Phys.: Condens. Matter **18** (2006) 6481–6492 doi:10.1088/0953-8984/18/28/004

Dynamic crossovers and activated regimes in a narrow distribution poly(n-butyl acrylate): an ESR study

Laura Andreozzi[1], **Ciro Autiero, Massimo Faetti, Marco Giordano and Fabio Zulli**

Department of Physics 'E Fermi', University of Pisa, largo Pontecorvo 3, 56127 Pisa, Italy
and
polyLAB-CNR, largo Pontecorvo 3, 56127 Pisa, Italy

E-mail: laura.andreozzi@df.unipi.it

Received 24 October 2005, in final form 12 April 2006
Published 28 June 2006
Online at stacks.iop.org/JPhysCM/18/6481

Abstract

The rotational dynamics of the spin probe cholestane dissolved in a narrow distribution poly(n-butyl acrylate) sample has been investigated via electron spin resonance (ESR) spectroscopy. The measurements were carried out in a wide temperature range: different dynamic regions have been recognized, and the coupling of the probe dynamics to the α and secondary relaxations has been revealed. In particular, the coupling with the structural relaxation is ruled by two fractionary Vogel–Fulcher laws (VF). The crossover from one VF region to the other occurs at the temperature $T_C = 1.17T_g$, signalling the onset of the cooperativity in the dynamics and confirming a behaviour previously observed in ESR studies carried out on polymeric glass-formers. Furthermore, in this work we discuss the activated regime at the highest temperatures and show that the activation energy does not depend on the length of the polymer main- and side-chains, while its onset temperature linearly depends on the chain length.

1. Introduction

Advanced comprehension of the mechanisms of relaxation in glass-forming materials in their supercooled state is a challenging topic in condensed matter physics. In particular, the occurrence of non-exponential and non-Arrhenian character in the structural relaxation is not thoroughly understood at the moment [1, 2]. The latter is usually described in terms of the Vogel–Fulcher (VF), or the Williams–Landel–Ferry (WLF) [3, 4], temperature scaling. However, often a single set of VF/WLF parameters is not able to account for the experimental α relaxation data. More generally there is a lot of experimental evidence for the occurrence of dynamic changes or peculiarities taking place in a narrow range of temperatures typically located at about (1.1–1.2) T_g [5–10]. Also theoretical works predict the existence of a dynamic

[1] Author to whom any correspondence should be addressed.

crossover well above the calorimetric T_g [11, 12]. Enhanced diffusion, splitting of α and β relaxations, and changes in the VF/WLF parameters have been found with different techniques. These phenomena were ascribed to the onset of cooperative molecular rearrangements, and to the effect of the dynamic heterogeneity developing on approaching the glass transition from above. When polymeric materials are considered, polydispersity and entanglement could also play important roles.

Several experimental works have suggested that the lengthscale characterizing the heterogeneity and the cooperative regions is of the order of a nanometre [13].

This fact represents one of the reasons of the appeal of molecular probe spectroscopies to investigate polymer dynamics in this crossover region. Actually, through time resolved fluorescence measurements of doped malachite green molecules dissolved in different glass formers, there was found at temperatures near $1.2T_g$ a dynamic crossover below which the temperature dependence of the non-radiative decay time became smoother [7]. Similarly, positron annihilation lifetime spectroscopy studies [14] revealed a kink in the temperature dependence of the free volume expansion coefficient, located in the range $1.15–1.4T_g$.

As far as the study of this crossover region is concerned, electron spin resonance spectroscopy (ESR) deserves consideration due to its well known sensitivity on the nanometre lengthscale and nanosecond timescale. ESR investigations of the rotational dynamics of different paramagnetic tracers dissolved in low molecular weight glass formers [15–17] evidenced the existence, in the supercooled region, of partial coupling between probe rotation and shear viscosity. Such a coupling was expressed in terms of a power law $\tau_c = c(\eta/T)^{\xi}$, τ_c being the rotational correlation time of the probe. A value of the exponent ξ other than unity was ascribed to the occurrence of cooperative phenomena. More complex scenarios were found by investigating the rotational dynamics of tracers dissolved in polymers, where careful analyses of the ESR lineshapes allowed one to evidence the effects of dynamic heterogeneity in different systems. These were related to the presence of continuous [18] or discrete [19] distributions of molecular sites available to probe rotation depending either on the polydispersity index, the thermal treatment or the presence of plasticizing impurities. On the other hand, a homogeneous character of the tracer reorientation was observed in almost monodisperse poly(ethylacrylate) (PEA) syntheses [8]. In spite of the quite different polymeric systems investigated, a dynamic crossover located at about $1.2T_g$ was evidenced in many studies [8, 18, 19]. At such a temperature a kink in the temperature dependence of the rotational correlation times was observed that was related to the occurrence of a larger decoupling from the structural relaxation of the host matrix.

In this work, the temperature dependence of the rotational dynamics of the cholestane spin probe dissolved in a narrow distribution poly(n-butyl acrylate) (PnBA) sample has been investigated by means of ESR spectroscopy. The coupling degree of the probe dynamics to the structural relaxation, the onset of cooperativity, and the crossover to activated regimes are topics of interest in the present study.

1.1. ESR spectroscopy: theoretical background

In X-band ESR experiments, a static magnetic field defining the z-axes of the laboratory frame resolves the Zeeman degeneracy of the spin system, whereas a microwave field ($\nu \approx 10^{10}$ Hz) linearly polarized along the x-axis induces σ transitions among the Zeeman levels. The quantity that is detected by the ESR spectroscopy is the transverse component of the ensemble magnetization, M_x. In particular, if the irradiating microwave power is low enough, the linear response theory [20] can be employed and the ESR lineshape $L(H_0)$ can be expressed in terms of the Laplace transform of the time correlation function of M_x [21]:

$$L(H_0) = C\frac{\partial}{\partial H_0}\mathrm{Re}\int_0^\infty \langle M_x M_x(t)\rangle \mathrm{e}^{\mathrm{i}\gamma H_0 t}\,\mathrm{d}t. \tag{1}$$

In this equation C is a constant, $\mathrm{i} = \sqrt{-1}$, Re (z) means the real part of z and the presence of the derivative is due to the phase detection of the ESR signal. The lineshape depends on the rotational dynamics of the spin system because the principal magnetic interactions, namely the Zeeman and the hyperfine ones, are anisotropic in character with their principal axes that are fixed in a molecular frame, whereas the spin is quantized along the z-axes of the laboratory frame. So the reorientation mechanism of the paramagnetic system results in fluctuating local magnetic fields, which relax the magnetization and broaden the resonance. This can be formalized by recognizing that the relevant spin Hamiltonian for diluted paramagnetic probes dissolved in host diamagnetic matrices can be expressed as

$$H = H_\mathrm{s} + H_\mathrm{sB} + H_\mathrm{B}. \tag{2}$$

H_s is the Hamiltonian independent of the probe reorientation, H_B represents the lattice Hamiltonian describing the rotational degrees of freedom of the thermal bath and H_sB couples the spin and orbital variables. The rotational dynamics is described in terms of proper stochastic processes [22, 23], by expanding the conditional probability for the molecular orientation $P(\Omega, t|\Omega_0, t_0)$ in terms of Wigner matrices [24]. The analysis of the ESR spectra is well established [21, 25–27]. Different approaches are employed in order to reproduce the ESR lineshapes according to equation (1), depending on the timescale of the spin probe rotation. When the rotational dynamics of spin probes is fast enough, the fluctuating local magnetic fields are rapidly averaged out and all spins behave in a similar way. The lineshape consists of $2I + 1$ (I being the nuclear spin of the probe) Lorentzian resonance peaks and the dynamic information is entirely contained in the linewidths. A second order perturbative scheme based on a coarse grained procedure can be used in this fast motion region [26–28]. The linewidths are expressed in terms of the spectral density power of the local fields, namely the Fourier transform of the autocorrelation functions of Wigner matrices of rank two, evaluated at zero frequency (secular terms) and at the characteristic frequencies of the spin systems defined by the isotropic part of the Zeeman (ω_0) and hyperfine (ω_I) interactions.

When the rotational dynamics of the probes becomes slower and slower the perturbative scheme of the fast motion regime cannot be used and more complex strategies are necessary to solve equation (1) numerically. Different algorithms have been developed in the literature [21, 29, 30] that are based on the stochastic Liouville method [31]. According to this method, the rigorous Liouvillian superoperator of the system which drives the time evolution of the observables, $\mathrm{i}L = \mathrm{i}H^X = -\mathrm{i}[H, \ldots]$, is replaced with the dynamical operator

$$\Gamma = \mathrm{i}H_\mathrm{s}^x + \mathrm{i}H_\mathrm{sB}^x + \Gamma_\Omega^+ \tag{3}$$

where Γ_Ω^+ is the operator adjoint to the stochastic operator Γ_Ω introduced in the master equation describing the reorientational process [22, 23]:

$$\frac{\partial P(\Omega, t|\Omega_0, t_0)}{\partial t} = \Gamma_\Omega P(\Omega, t|\Omega_0, t_0). \tag{4}$$

In this framework, Freed and co-workers [32] were the first to evidence the great sensitivity of the ESR lineshapes to the details of the molecular reorientation. A very fast and powerful algorithm to evaluate slow motional ESR lineshapes by means of equations (1) and (3) was then developed by Giordano and co-workers [21] by using the generalized Mori projection technique [33]. Accordingly, the ESR spectrum is written as a continued fraction whose terms can be evaluated by means of an iterative scheme where the superoperator Γ of equation (3) is let to act on a proper biorthogonal set of base vectors containing spin operators and Wigner matrices. In this way it is easily shown that the computed lineshape, depending on the

autocorrelation functions of Wigner matrices of different even rank, allows one to discriminate among different stochastic models of reorientation, namely simple diffusion, jump dynamics and so on [32, 34].

On further slowing down of the molecular reorientation the rigid limit is reached where the ESR lineshape is unaffected by the spin probe rotation and can be reproduced by adding the responses of the single spin packets with fixed orientation randomly distributed over the solid angle. In the high field approximation valid for ESR in X-band, each spin packet contributes with $2I+1$ resonance lines located at frequencies depending on the orientation in a quite simple way [35]. The accurate analysis of the rigid spectrum, that is usually referred to in the literature as a *powder spectrum*, is of fundamental importance because it allows the evaluation of the components of the Zeeman and hyperfine tensors (magnetic parameters) that can be reasonably considered temperature independent [32].

1.2. Timescales

As already stated, the ESR lineshape is strongly dependent on the motional regime of the spin probes, and three different dynamic regimes are identified as fast, slow and ultraslow motion regimes. The values of reorientational correlation times falling in these different regions are naturally related to the value of the static magnetic field and to the magnetic parameters of the specific spin probe adopted. We discuss here only the X-band ESR spectroscopy of nitroxide spin probes. In such a case the relevant timescale extends for some decades around the nanosecond, roughly in the range 10^{-12}–10^{-6} s. More particularly, when the correlation time falls in the range 10^{-12} s $< \tau_c <$ 10^{-9} s the ESR spectra show the typical $2I + 1$ Lorentzian shape of the fast motion regime with the dynamic information contained in the linewidths. When τ_c approaches a nanosecond, the lineshape begins to show more complex patterns typical of the slow motion regime. For $\tau_c \sim 10^{-8}$ s the ESR lineshape evidences the strongest temperature dependence, whereas when τ_c becomes longer than 10^{-7} s the spectra appear, at a first glance, to be almost temperature independent. However, fixing the limit where the ultraslow motion regime really sets in is not simple, and the values of 10^{-7} or 10^{-6} s that can be found in the literature are only indicative. Actually, works have been published where correlation times of some microseconds or more have been obtained [36, 37]. In fact, a rigorous powder spectrum is present only when the lineshape is completely independent of the spin probe motion. On the other hand, when the rigid limit is approached the ESR spectrum shows two outer hyperfine extrema arising from those radicals for which the 2p π molecular orbital of the NO moiety is nearly parallel to the static magnetic field. The shape and the spectral separation of these extrema, referred to in the literature as $2A_{zz}$, is very strongly dependent on the residual motion. A long time ago, through an analysis of these outer hyperfine peaks, Freed [38] developed a semiempirical experimental procedure allowing the measure of correlation times longer than 10^{-6} s. Regarding the measurements of the present work, given the high stability of the static magnetic field and the sensibility of the Bruker ER035M gaussmeter, a spectral resolution of the order of 10^{-2} gauss can be reached. In this way it is possible to reproduce with such a precision the positions of the two outer extrema and to follow the dynamics of spin probe when the correlation time is of the order of some microseconds with an error less than 20%. In this study we adopted this high resolution procedure on cooling starting from about 20 K above T_g.

1.3. Lengthscales

Similarly to other probe spectroscopies, the lengthscale relevant to the ESR experiments is related the size of the adopted paramagnetic tracer. In the last few years, we used two different

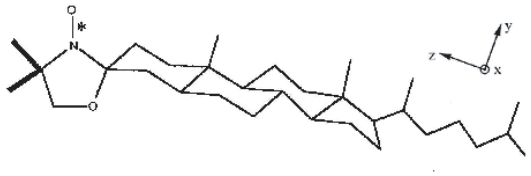

(a)

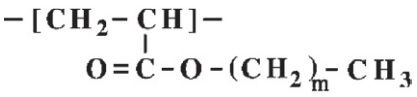

(b)

Figure 1. (a) Molecular structure of the cholestane spin probe and principal axes of the molecular frame. (b) Repeating unit of the poly(alkyl acrylate)s. Poly(n-butyl acrylate) and poly(ethyl acrylate) are represented by setting $m = 3$ and $m = 1$ respectively.

nitroxide radicals to investigate polymer dynamics: the smaller tempo probe and the larger cholestane. The former is almost spherical in shape with a van der Waals radius of 0.34 nm, whereas the latter is cigar-like shaped with semiaxes of about 1 and 0.3 nm respectively. Their sizes are just across the nanometre lengthscale that, according to all the recent experiments, characterizes the dynamic heterogeneity and cooperativity in polymers and supercooled liquids.

It is sometimes believed that for studying polymer dynamics through probe spectroscopies, the size of the probe should be small enough to provide good spatial resolution. At variance with this statement, probes too small can provide results strongly dependent on the specific peculiarity of the tracer–polymer interaction. In fact for the case of the spin probe tempo our studies evidenced different scenarios: in poly(vinyl acetate) (PVAc) [18] the tracer dynamics was strongly coupled to the relaxation processes of the host, tracking the α, β and γ dielectric relaxation processes on decreasing the temperature, whereas in a synthesis of polystyrene (PS) [39] we found quite similar ESR spectra in a very broad temperature range evidencing a large decoupling between tracer and host dynamics. Similar results were found by comparing the dynamics of tempo probe in several polymers [40].

In contrast, the larger probe cholestane evidenced a common dynamic behaviour in different polymers [8, 19, 41]. In particular the tracer dynamics was found to be partially coupled to the dynamics of the host with the possibility of expressing its coupling in terms of a power law $\tau_c = c(\eta/T)^{\xi}$ with $0 < \xi < 1$. Furthermore, a sharp dynamic change between two power law regimes was evidenced well above the glass transition temperature. Such a crossover took place at temperatures located in the range $1.1T_g$–$1.2T_g$ where, according to a large amount of experimental data [6], different types of dynamic crossover are observed depending on the polymer and on the experimental technique.

Finally, near to the glass transition temperature the tracer dynamics became activated. In the present study it has been found that the cholestane rotational dynamics in PnBA followed this general scenario.

2. Materials and experimental details

The molecular structure of the repeating unit of PnBA is shown in figure 1. The PnBA polymer was purchased by PolymerSource Inc. (Montreal, Canada), who provided the molar mass data from size exclusion chromatography using polystyrene standards. The molar mass of the sample was smaller than the entanglement mass M_e of the polymer ($M_w \leqslant M_e$ [42]). The glass transition temperature was obtained from differential calorimetry scans carried out with a Perkin Elmer DSC7 apparatus calibrated with indium and zinc standards. Thermograms were recorded on heating at 10 K min^{-1} after quenching at 40 K min^{-1}. The linear viscoelastic

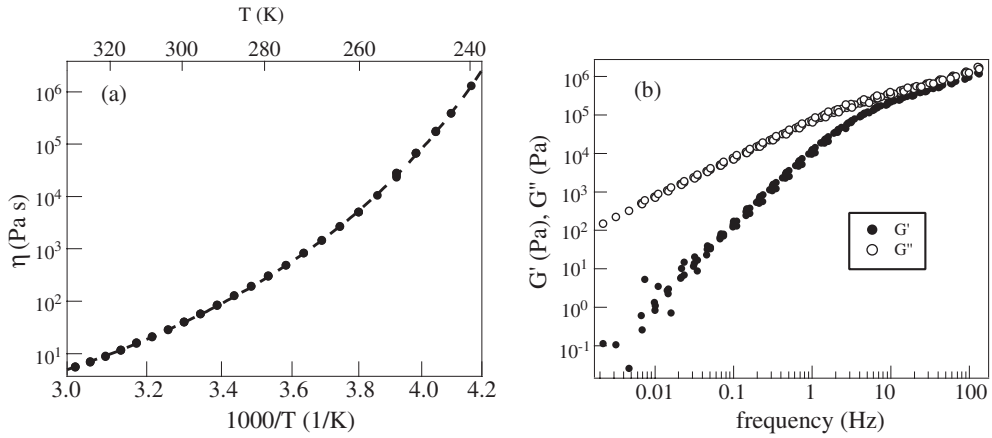

Figure 2. (a) Temperature dependence of the zero-shear viscosity of PnBA. (b) Master curve of PnBA at the reference temperature $T_r = 259$ K.

Table 1. Characterization data for the PnBA sample.

M_n (g mol^{-1})	M_w (g mol^{-1})	M_w/M_n	T_g (K)	η_∞ (Pa s)	T_b (K)	T_0 (K)
13 000	14 700	1.13	224 ± 1	$(6.6 \pm 0.2) \times 10^{-4}$	1425 ± 30	174 ± 3

response of the PnBA polymer melt was investigated by means of a Haake RS150 rheometer in the temperature range 239–340 K by oscillatory measurements from 10^{-2} to 24.4 Hz, and creep and flow experiments. The zero-shear viscosity η was found to follow the Vogel–Fulcher (VF) law:

$$\eta = \eta_\infty \exp\left(\frac{T_b}{T - T_0}\right); \tag{5}$$

T_b is the pseudo-activation energy expressed in kelvin, and T_0 the Vogel temperature. Figure 2(a) shows the temperature dependence of the zero-shear viscosity. Figure 2(b) gives the master curve obtained by superimposing the curves $G'(\omega)$ and $G''(\omega)$ of PnBA measured at different temperatures. The data were shifted along the logarithmic frequency axis with respect to the reference temperature of $T_r = 259$ K, following the time–temperature superposition principle [4]. Accordingly, PnBA was a thermorheologically simple polymer also in agreement with literature studies [42]. No evidence of a rubbery plateau was found, as expected for unentangled polymers. In the lowest frequency region, the curves show the behaviour of monodisperse linear polymers: $G' \propto \omega^2$ and $G'' \propto \omega$. Molar masses and physico-chemical quantities relevant to the thermo-rheological characterization as T_g, T_b, T_0, and η_∞ are given in table 1.

ESR studies were performed by using an X-band Bruker ER 200 SRC spectrometer equipped with a Bruker BVT100 temperature control apparatus with nominal accuracy of ± 0.1 K. The cholestane nitroxide (3[beta]-doxyl-5[alpha]-cholestane, 98%, figure 1) was used as received from Sigma-Aldrich (Milan, Italy). Samples were prepared by mixing two chloroform solutions containing predetermined amounts of polymer and cholestane. The resulting solution (1.4×10^{-4} mol/repeating unit) was evaporated to complete dryness by being heated to 358 K under vacuum for about 120 h, and finally sealed in a standard ESR tube. The principal components of magnetic tensors of the spin probe in PnBA were drawn by the powder

Table 2. Values of the components of the Zeeman and hyperfine tensors in the principal molecular reference frame of cholestane in PnBA.

g_{xx}	g_{yy}	g_{zz}	a_{xx} (G)	a_{yy} (G)	a_{zz} (G)
2.0033	2.0092	2.0071	33.3	6.2	4.0

Table 3. Molar mass M_w, polydispersity M_w/M_n, number of repeating units M_w/M_0, and glass transition temperature T_g for PEA samples. M_0 is the molar mass of the PEA repeating units.

M_w (g mol^{-1})	M_w/M_n	M_w/M_0	T_g (K)
13 100	1.13	131	252 ± 1
9 600	1.09	96	250 ± 1
8 250	1.10	82	248 ± 1
7 800	1.07	78	247 ± 1

ESR spectrum recorded at 140 K, according to a procedure detailed elsewhere [35]. The values, in the molecular frame, of the Zeeman and hyperfine tensors are listed in table 2.

Due to the polymer viscosity, the spin probe rotation falls in the ESR slow motion regime, where the spectroscopy exhibits enhanced sensitivity to details of the molecular dynamics. The dynamic information is evaluated from the ESR experimental lineshape by numerical simulation based on the generalized Mori theory [21, 33]. As found in other polymers, the reorientation mechanism of the probe was conveniently described by the diffusion model [43]. In particular, due to its nearly axial symmetry, the cholestane spin probe exhibits an anisotropic reorientational dynamics. Hence, the motion of the molecular tracer is characterized by spinning and tumbling rotation with correlation times $\tau_\parallel$ and $\tau_\perp$ respectively. In this paper, the rotational dynamics of cholestane in PnBA at the highest investigated temperatures will be compared with that of a set of narrow distribution PEA samples with different masses. PEAs were synthesized [8] following a controlled/living radical polymerization, by the ATRP technique, given in the literature. The preparation and the characterization of these samples followed the same procedure used for PnBA and detailed above. In table 3 data for the mass distribution and the glass transition temperature are given.

3. Results and discussion

The ESR measurements on PnBA were carried out in the temperature range 394–205 K. Figure 3 shows the good agreement between some representative experimental ESR spectra recorded at different temperatures and the corresponding theoretical lineshapes. From these experiments the values of $\tau_\parallel$ and $\tau_\perp$ are drawn in the whole investigated temperature interval. The temperature dependence of the anisotropy ratio $\tau_\perp/\tau_\parallel$ ranges from 12 to 20.

Figure 4 shows the dependence of the spinning time $\tau_\parallel$ of cholestane in PnBA, versus $1000/T$. Five dynamic regions can be identified. The temperature dependence of the correlation time in each region is well reproduced by assuming either Arrhenius (Arrh) behaviour:

$$\tau_\parallel = \tau_{\parallel\infty} \exp\left(\frac{\Delta E}{k_B T}\right), \tag{6}$$

or Vogel–Fulcher (VF) behaviour:

$$\tau_\parallel = \tau_{\parallel\infty} \exp\left(\frac{T_b}{T - T_0}\right). \tag{7}$$

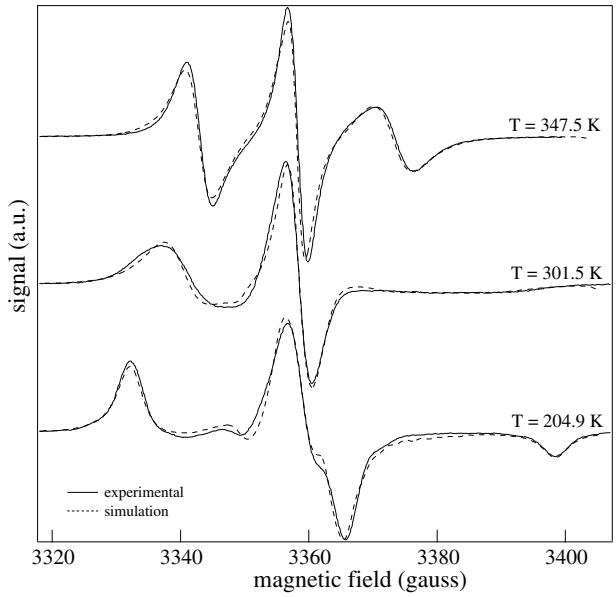

Figure 3. Examples of ESR experimental spectra and their simulations for the cholestane probe in PnBA.

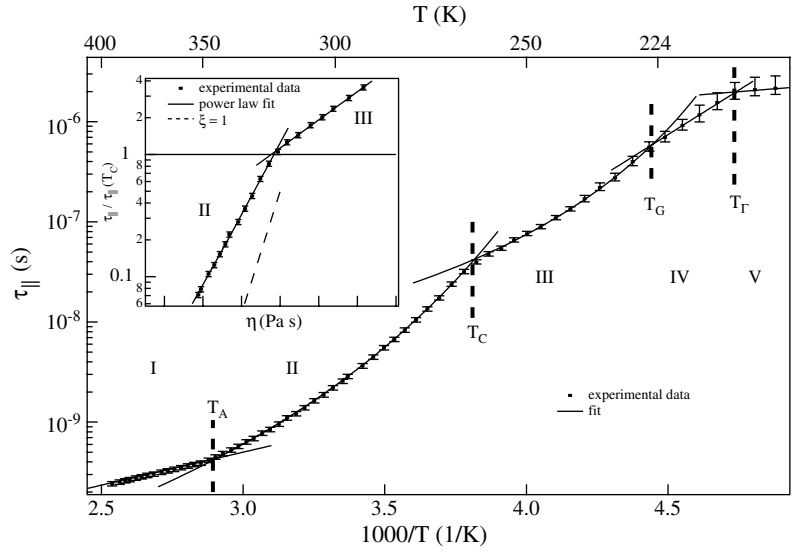

Figure 4. Temperature dependence of the spinning correlation time of the cholestane spin probe dissolved in PnBA. The superimposed curves are the VF (regions II and III) and Arrh (regions I, IV and V) laws. Inset: fractional coupling between $\tau_{\|}$ and η in the dynamic regions II and III (see equation (8)). The dashed line corresponds to $\xi = 1$.

The parameters pertinent to the different dynamic regimes are given in table 4.

First, let us consider the two dynamic regions II and III, where the temperature dependence of the molecular spinning time shows a crossover from one VF law to another one. In both temperature regions, the Vogel temperature T_0 has the same value as that of the rheological

Table 4. Fit parameters for the temperature dependence of the spinning correlation time of cholestane in PnBA.

Zone	Temperature range (K)	Relaxation	Fit law	ΔE (kJ mol^{-1})	T_b (K)	T_0 (K)
I	$345 \pm 2 = T_A < T$		Arrh	12.6± 1.6	—	—
II	$262 \pm 2 = T_C < T < T_A = 345 \pm 2$	α	VF	—	820 ± 40	175 ± 5
III	$225 \pm 2 = T_G < T < T_C = 262 \pm 2$	α'	VF	—	310 ± 20	175 ± 5
IV	$211 \pm 2 = T_\Gamma < T < T_G = 225 \pm 2$	γ	Arrh	33 ± 3	—	—
V	$T < T_\Gamma = 211 \pm 2$		Arrh	4.3 ± 0.8	—	—

measurements (table 1); therefore $\tau_\parallel$ can be expressed in terms of a fractionary law of the viscosity η:

$$\tau_\parallel \propto [\eta(T)]^\xi. \tag{8}$$

In equation (8), the fractionary exponent ξ may vary between 0 and 1, with $\xi = 1$ corresponding to a complete coupling of the probe dynamics to the structural relaxation of the host matrix. The fractional exponent is the ratio of the pseudo-activation energy T_b of the VF followed by the probe rotation (table 4) to the T_b pseudo-activation energy of the structural relaxation given in table 1. The inset of figure 4 magnifies the crossover between region II and III evidencing the ability of equation (8) to describe the experimental data in these two regions. Values $\xi = 0.57 \pm 0.03$ and $\xi = 0.21 \pm 0.02$ are found in the dynamic regions II and III respectively. The existence of the fractional coupling of equation (8) proves the probe and host compatibility.

In [19] the decoupling of the dynamics of a tracer dissolved in a side chain liquid crystal methacrylate homopolymer was observed in a temperature region corresponding to the current dynamic region II and was ascribed to a steric hindrance due to the specific characteristic of the host matrix. The further decoupling of the probe dynamics from the α relaxation of the polymer host observed in that work on lowering the temperature was taken as a signature of the onset of cooperative processes in the polymeric matrix. The ratio ξ_C of the fractional exponent of the intermediate temperature region to the high temperature region one resulted in being an evaluation of the cooperative probe dynamics occurring in region III itself, and the value $1/\xi_C$ an evaluation of the number of cooperative units of the polymeric matrix as estimated on the lengthscale of the molecular probe. In the present study on PnBA, the crossover from dynamic region II to III occurs in a way very similar to that also observed in [8], where the cholestane spin probe dissolved in two PEA samples with different molar masses had been studied. The onset of cooperative phenomena was located at $T_C/T_g = 1.14$ for PEA with $M_n = 7500$ g mol^{-1}, and $T_C/T_g = 1.19$ for PEA with $M_n = 58\,200$ g mol^{-1}. Here, on PnBA, the crossover temperature has been found at $T_C = 1.17T_g$, in agreement with the value range of the critical temperature (1.1–$1.2T_g$) foreseen by the mode-coupling theory of the glass transition [12]. Intriguingly enough, such a finding is common to different samples [8, 18, 19, 41], and has also been revealed with different spectroscopies [5–7, 44]. Moreover, the size of the rearranging cooperative regions of the host, evaluated via the quantity $1/\xi_C = 2.6$, compares with the value of 2.5 found in [8] for PEA samples with molar mass both smaller and greater than the entanglement mass.

From an inspection of figure 4, the value of the spinning correlation time at the crossover is $\tau(T_C) = 3.7 \times 10^{-8}$ s. It results in the same order of magnitude of the monomeric rotational correlation time τ_m as found from measurements of nuclear magnetic resonance on polybutadiene [45]. That study provided τ_m as molar-mass independent, with a value of about 10^{-8} s. A value of $\tau(T_C) \approx 3 \times 10^{-8}$ s has also been found for entangled and unentangled

Table 5. Number of repeating units M_w/M_0 (M_0 is the molar mass of the repeating units), glass transition temperature T_g, energy of activation ΔE_h, and onset temperature T_A of region I for PEA and PnBA samples.

Sample	M_w/M_0	T_g (K)	ΔE_h (kJ mol^{-1})	T_A (K)
PnBA	115	224 ± 1	12.6 ± 1.6	345 ± 2
PEA	131	252 ± 1	13 ± 3	396 ± 3
PEA	96	250 ± 1	12.6 ± 1.6	369 ± 2
PEA	82	248 ± 1	12.6 ± 1.6	355 ± 2
PEA	78	247 ± 1	12.7 ± 1.6	353 ± 2

PEAs independently of the molar mass [8]. Nevertheless, a weak dependence on the side-chain structure can be observed on examining the τ_m data obtained from PEA and PnBA samples: the bigger the monomeric unit, the slower the reorientational dynamics.

At lower temperature, a crossover to an activated regime occurs at $T_G = 225$ K, practically coincident with the calorimetric glass transition temperature of PnBA (table 1). The values of the activation energy in region IV, $\Delta E_\gamma = 33$ kJ mol^{-1}, suggest that the rotational dynamics is coupled to the γ relaxation process of the polymeric matrix. In fact, this value of ΔE_γ agrees very well with the activation energy ΔE_γ of secondary γ relaxation of 31 kJ mol^{-1} found via dielectrometric measurements for PnBA [46, 47]. The γ relaxation for poly(alkyl acrylate)s is supposed to involve limited movements inside the −COOR side chains [46, 48].

A further dynamic regime takes place at even lower temperatures (region V). There the probe rotation is coupled to the more local relaxation processes [18]. In fact, the value of the activation energy of the process, $\Delta E = 4.3 \pm 1.2$ kJ mol^{-1}, is comparable to the barrier height between gauche and trans sites around the O–C bonds of the side-chain ester group, according to a calculation carried out in [46].

Finally, let us focus our attention on the very high temperature region above 345 K (region I), where an Arrhenius dynamic behaviour is observed. This activated regime has $\Delta E_h = 12.6$ kJ mol^{-1}, which is a value comparable with those found in simple fluids and polymers [49, 50]. This region also has been recently found in other polymers [8]. A comparison between this dynamic behavior in unentangled PEA samples and PnBA is presented here. Table 5 reports the energy of activation, ΔE_h, and the onset temperature, T_A, of region I for PEA and PnBA samples.

As one can see from table 5, the value of the energy of activation for PEA and PnBA samples is constant, with dependence neither on the length of the main chain nor on the side chain. In literature studies, this effect has been attributed [50] to a configurational change of conformers along the main chain when they are able to rotate without being interfered with by their neighbours. The relaxation time has been found to range from 10^{-10} to 10^{-12} s [51], in nice agreement with the values of the spinning correlation time of cholestane in region I. A constant value of $\approx$12.6 kJ mol^{-1} for the energy of activation of such a conformational relaxation has been found in theoretical studies [51]. This value agrees well with those found by ESR and reported in table 5.

Even if the mechanism driving the dynamics is not cooperative, the onset temperature is related to the main chain length: in fact, the longer the chains, the higher the onset temperature. This should be expected considering that the phenomenon is isoviscous; for all the investigated samples $\eta(T_A) \approx 2$ Pa s. This value therefore seems to be the maximum zero-shear viscosity allowed for the chain torsion. On the other hand, the presence of entanglement may fake this effect as observed in a previous work on PEA [8]. In figure 5, the T_A/T_g values are plotted against the number of repeating units of the chain (M_w/M_0, where M_0 is the molar mass of the

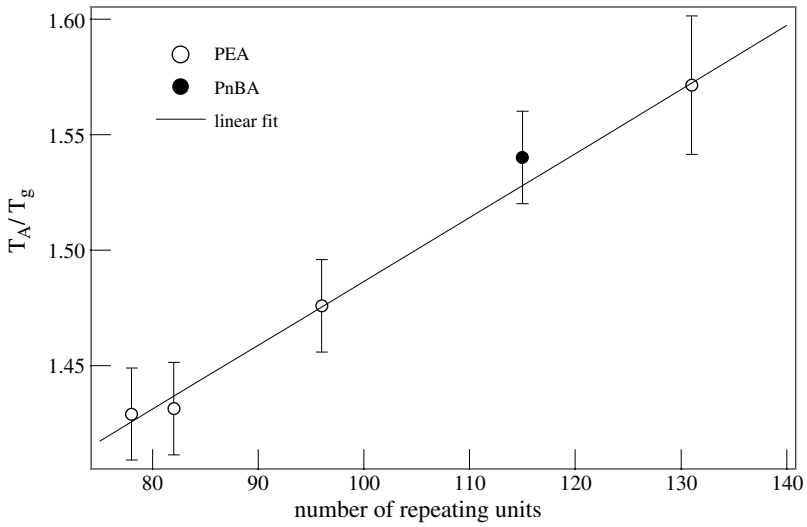

Figure 5. Ratio T_A/T_g as a function of the number of repeating units of the PEA and PnBA samples.

repeating unit). A linear fit

$$\frac{T_A}{T_g} = A + B\frac{M_w}{M_0} \tag{9}$$

provides the values $A = 1.22 \pm 0.01$, $B = 0.0027 \pm 0.0001$, and $\chi^2 = 0.67$.

4. Conclusions

The rotation of the cholestane tracer dissolved in a narrow distribution PnBA has been studied in a large temperature interval. The probe dynamics shows different regimes with sharp crossovers, and it tracks the relaxation mechanisms of the host. Activated regimes in low temperature regions appear to be coupled to secondary relaxation processes of the polymer matrix. Above the glass transition temperature, scaling laws of the structural relaxation are followed, providing information on the occurrence of cooperative processes in PnBA at the timescale/lengthscale of the molecular probe. These studies, also to be carried out at different timescales/lengthscales, have recently been evaluated [52] as most useful for understanding cooperativity and dynamic heterogeneity in supercooled fluids. Finally, an activated regime above the onset temperature T_A has been recognized to be due to conformer transitions along the main chain of the polymer. The finding was compared with similar activated high temperature regimes observed in a series of unentangled PEAs with variable masses. Interestingly enough, the onset of the conformer rotation appears to be an isoviscous phenomenon.

Acknowledgment

This work was partially supported by Italian MIUR and INFM Pais project.

References

[1] Ngai K L 2000 *J. Non-Cryst. Solids* **275** 7–51
[2] Angell C A, Ngai K L, McKenna G B, McMillan P F and Martin S W 2000 *J. Appl. Phys.: Appl. Phys. Rev.* **88** 3113–57

[3] Vogel H 1921 *Z. Phys.* **22** 645
Fulcher G S 1925 *J. Am. Ceram. Soc.* **8** 339
[4] Ferry J D 1980 *Viscoelastic Properties of Polymers* 3rd edn (New York: Wiley)
[5] Donth E 2001 *The Glass Transition* (Berlin: Springer)
[6] Beiner M, Huth H and Schröter K 2001 *J. Non-Cryst. Solids* **279** 126–35
[7] Ye J Y, Hattori T and Nakatsuka H 1997 *Phys. Rev.* B **56** 5286
[8] Andreozzi L, Faetti M, Giordano M, Zulli F and Castelvetro V 2004 *Phil. Mag.* **84** 1555–65
[9] Jin X, Zhang S H and Runt J 2004 *Macromolecules* **37** 8110–5
[10] Lorthioir C, Alegría A and Colmenero J 2003 *Eur. Phys. J.* E **12** S127–30
[11] Guenza M 2002 *Phys. Rev. Lett.* **88** 025901
[12] Götze W 1999 *J. Phys.: Condens. Matter* **11** A1–46
[13] Sillescu H 1999 *J. Non-Cryst. Solids* **243** 81–108
[14] Bartos J, Sausa O, Bandzuch P, Zrubcová J and Kristiak J 2002 *J. Non-Cryst. Solids* **307–310** 417
[15] Andreozzi Di Schino A, Giordano M and Leporini D 1997 *Europhys. Lett.* **38** 669
[16] Andreozzi L, Bagnoli M, Faetti M and Giordano M 2002 *J. Non-Cryst. Solids* **303** 262
[17] Andreozzi L, Faetti M and Giordano M 2006 *J. Phys.: Condens. Matter* **18** 931–40
[18] Faetti M, Giordano M, Leporini D and Pardi L 1999 *Macromolecules* **32** 1876
[19] Andreozzi L, Faetti M, Giordano M, Palazzuoli D and Galli G 2001 *Macromolecules* **34** 7325
[20] Kubo R, Toda M and Hashitsume N 1985 *Statistical Physics* vol 2 (Berlin: Springer)
[21] Giordano M, Grigolini P, Leporini D and Marin P 1985 *Adv. Chem. Phys.* **62** 321
[22] Van Kampen N G 1981 *Stochastic Processes in Physics and Chemistry* (Amsterdam: North-Holland)
[23] Gardiner C W 1985 *Handbook of Stochastic Methods* 2nd edn (Berlin: Springer)
[24] Rose M E 1957 *Elementary Theory of the Angular Momentum* (New York: Wiley)
[25] Muus L T and Atkins P W (ed) 1972 *Electron Spin Relaxation in Liquids* (New York: Plenum)
[26] Berliner L J (ed) 1976 *Spin Labelling: Theory and Applications* vol 1 (New York: Academic)
Berliner L J (ed) 1979 *Spin Labelling: Theory and Applications* vol 2 (New York: Academic)
[27] Slichter C P 1965 *Principles of Magnetic Resonance* (New York: Harper&Row)
[28] Redfield A G 1957 *IBM J. Res. Dev.* **1** 19
[29] Korst N N and Lazarev A V 1969 *Mol. Phys.* **17** 481
[30] Freed J H, Bruno G V and Polnaszek C F 1971 *J. Phys. Chem.* **75** 3385
[31] Kubo R 1969 *J. Phys. Soc. Japan* **26** (Suppl.) 1
[32] Goldman S A, Bruno G V, Polnaszek C F and Freed J H 1972 *J. Chem. Phys.* **56** 716
[33] Grigolini P 1985 *Memory Functions Approaches to Stochastic Problems in Condensed Matter* ed M W Evans, P Grigolini and G Pastori Parravicini (New York: Wiley)
[34] Andreozzi L, Bagnoli M, Faetti M and Giordano M 2002 *Phil. Mag.* B **82** 409
[35] Andreozzi L, Giordano M and Leporini D 1993 *Appl. Magn. Res.* **4** 279
[36] Shiotani M, Moro G and Freed J H 1981 *J. Chem. Phys.* **74** 2616
[37] Hwang J S, Mason R P, Hwang L P and Freed J H 1975 *J. Phys. Chem.* **79** 489
[38] Mason R P and Freed J H 1974 *J. Phys. Chem.* **78** 1321
[39] Andreozzi L, Autiero C, Faetti M, Giordano M and Zulli F 2006 unpublished results
[40] Bartos J and Hlouskova Z 1993 *Polymer* **34** 4570
[41] Andreozzi L, Faetti M, Giordano M, Palazzuoli D, Zulli F and Galli G 2005 *Mol. Cryst. Liq. Cryst.* **429** 21
[42] Ahmad N M, Lowell P A and Underwood S M 2001 *Polym. Int.* **50** 625
[43] Favro L D 1960 *Phys. Rev.* **119** 53
[44] Kisliuk A, Mathers R T and Sokolov A P 2000 *J. Polym. Sci.* B **38** 2785
[45] Guillermo A and Cohen Addad J P 2002 *J. Chem. Phys.* **116** 3141
[46] Hayakawa T and Adachi K 2000 *Polym. J.* **32** 845
[47] Gómez Ribelles J L, Meseguer Dueñas J M and Monleón P 1989 *J. Appl. Polym. Sci.* **38** 1145
[48] McCrum N G, Read B E and Williams G 1991 *Anelastic and Dielectric Effects in Polymeric Solids* (New York: Dover)
[49] Macosko C W 1994 *Rheology* (New York: Wiley) p 100
[50] Matsuoka S 1997 *J. Res. Natl Inst. Stand. Technol.* **102** 213
[51] Bovey F A and Winslow F H (ed) 1979 *Macromolecules* (New York: Academic) p 247
[52] Berthier L 2004 *Phys. Rev.* E **69** 020201 ®